Critical Slowing Down of Chemical Reactions in Liquid Mixtures

James K. Baird* and John C. Clunie

Department of Chemistry, University of Alabama in in Huntsville, Huntsville, Alabama 35899

Received: May 4, 1998

We have observed suppression in the specific rate of hydrolysis of five organic halides in three water-based liquid mixtures near their respective equilibrium consolute points. The systems examined were *tert*-amyl chloride in isobutyric acid + water, *tert*-butyl chloride in isobutyric acid + water, *tert*-butyl bromide in triethylamine + water, 3-chloro-3-methylpentane in 2-butoxyethanol + water, and 4-methylbenzylbromide in 2-butoxyethanol + water. The first two have upper consolute temperatures, while the second three have lower consolute temperatures. The slowing down effect occurred within a few tenths °C on either side of the consolute temperature. In the case of *tert*-amyl chloride in isobutyric acid + water, the effect followed a shift in consolute temperature produced by a change in the initial concentration of *tert*-amyl chloride. This indicates that all points along the critical line are equivalent. These observations demonstrate the existence of critical slowing down of chemical reaction rates in liquid mixtures.

Introduction

The point on the pressure−volume−temperature (P−V−T) surface of a pure fluid where the distinction between liquid and gas disappears is called the critical point. The fluid in the one-phase region above the critical point can be used as the solvent for various chemical reactions. Since the first examination of oxidation reactions by Toriumi *et al.*[1] and dimerization and atomic recombination reactions by Krichevskii and collaborators,[2−4] the field has greatly expanded to include, for example, complex formation, unimolecular decomposition, photoreduction, dehydrogenation, and pyrolysis. The detailed results have been frequently described and reviewed.[5−9]

When the solvent fluid consists of not one but two components, the coexistence curve expands to become a coexistence surface, while the critical point extends to become a line of critical points, each one corresponding to a different pressure. Two component mixtures at 1 atm pressure often have a liquid−vapor critical point (plait point) and often also a liquid−liquid critical point (consolute point). The consolute point is an extremum in the temperature vs mole fraction phase diagram where the homogeneous liquid solution first begins to separate into two immiscible liquid layers. A mixture of two components having a liquid−liquid phase boundary which is concave down is said to have an upper critical solution temperature (UCST), while one where the phase boundary is concave up is described as having a lower critical solution temperature (LCST). The presence of a liquid−liquid critical point recommends two-component mixtures as solvents for chemical reactions.[10] In contrast to pure fluids where the critical point ordinarily occurs at many atmospheres pressure, liquid mixtures can be used at atmospheric pressure. Moreover, a wide selection of liquid pairs is available. There are, for example, several thousand mixtures with an UCST and several hundred with an LCST.[11]

The theoretical concepts for exploiting critical point chemistry in mixed solvents have been discussed by Wheeler,[12] Milner and Martin,[13] Greer,[14] and Gitterman.[15] Although not in complete agreement on all points, the various theories suggest that in a system subject to a sufficient number of thermodynamic constraints, the position of chemical equilibrium should be shifted at the consolute point. This was confirmed in the case of the dimerization of NO_2 to N_2O_4 in perfluoromethylcyclohexane + carbon tetrachloride (UCST), where it was shown experimentally that there was a 4% shift toward the NO_2 side of the equilibrium as the consolute point was approached.[16]

Also given sufficient thermodynamic constraints, the rate of reaction in a fluid mixture is expected to be suppressed as the critical point is approached.[12−15] In 1973, Snyder and Eckert examined experimentally the disappearance of ethyl iodide on the one phase side of the LCST of triethylamine + water and reported an apparent slowing down in the rate near the consolute point.[17] Subsequently, Becker and collaborators[18] studied the trifluoroacetic acid catalyzed reaction of acetic anhydride + 1,2 ethanediol to form the 1,2 ester of ethanediol and acetic acid. In this case, the reacting pair (acetic anhydride + 1,2 ethanediol) also served as its own solvent. Following the reaction by calorimetry, Becker *et al.* reported that, near the consolute point, there was a decrease in the rate of heat evolution, which they associated with a slowing down in the rate of reaction of the solvent pair.

The observation of “critical slowing down” has not been universal, however. Snyder and Eckert reported an accelerated rate in the Diels−Alder addition of isoprene to maleic anhydride near the UCST of the two solvent pairs, hexane + nitrobenzene and hexane + nitroethane.[17]

Below, we report our measurements of the rates of hydrolysis of five organic halides dissolved in three different water-based solvent pairs. One of these pairs (isobutyric acid + water) has an UCST, while the other two (triethylamine + water) and (2-butoxyethanol + water) have LCSTs. In every case, we observed near the local consolute point a decrease in the specific rate of reaction. We believe that these observations conclusively demonstrate the phenomenon of critical slowing down of reaction rates in liquid mixtures.

Experimental Section

Table 1 summarizes the preparation of the reaction mixtures. The solvent pairs, isobutyric acid (IBA) + water,[19] triethylamine

S1089-5639(98)02105-7 CCC: $15.00

TABLE 1: Reactants and Mixed Solvents Demonstrating Critical Slowing Down of the Rate of Hydrolysis

solvent	wt %, T_c°(°C)	type	volume (mL)	reactant	amount	T_c(°C)
IBA + HOH	38.8, 26.2	UCST	25	tert-amyl chloride	0.100 mL	32.3
			25	*tert*-butyl chloride	1.00 mL	31.55
TEA + HOH	32.27, 18	LCST	25	*tert*-butyl bromide	0.100 mL	17.6
2BE + HOH	24.78, 49.0	LCST	25	3-chloro-3-methylpentane	0.300 mL	40.35
			30	4-methylbenzyl bromide	0.0730 g	44.3

(TEA) + water,[20] and 2-butoxyethanol (2BE) + water,[21] are listed in column one of the table, while their critical compositions and temperatures T_c° are listed in column two. The critical compositions are expressed in terms of the weight percent of the nonaqueous component. The third column identifies the consolute temperature as upper (UCST) or lower (LCST). The last four columns of the table refer to the mixture after introduction of the reactant. The fourth column gives the volume of solvent. The fifth and sixth columns, respectively, identify the reactant and list the amount used. In the seventh column, we report the consolute temperature T_c of the mixture at reaction equilibrium. Note that the introduction of the reactant always shifted the critical temperature of the mixture.[22] Visual observation of the disappearance of the meniscus was used to identify this temperature.

In the case of each mixture listed in Table 1, the hydrolysis of the halide RX

$$\mathrm{RX} + \mathrm{HOH} \rightarrow \mathrm{ROH} + \mathrm{HX} \qquad (1)$$

produced an alcohol, ROH, and an acid, HX, which was a strong electrolyte. The conductivity of the acid easily dominated any background conductivity due to the solvent. We thus could monitor the rate of reaction by following the rate of buildup of the conductivity of the solution. For this purpose, we used a radiometer (Copenhagen) model CDM 83 conductivity meter. The reaction mixture was contained in a test tube, which was large enough to accommodate the CDC immersion probe of this meter. The test tube and the probe were held at the desired temperature by placing them in a water bath controlled by a Philadelphia Roto-Stat differential thermoregulator connected to a Cole Parmer, 115 V Variable Output, Model G-02149-20 controller. The temperature was sensed with a Model S27929 L180 G(D), Serial No. 1516, platinum resistance thermometer supplied by Minco Products, Inc. The resistance of the thermometer was read using a Hewlett-Packard Model H3458A, $8^1/_2$ digit multimeter. Over a period of 2 h required to make each kinetics run, the temperature of the bath was stable to ±0.3 mK.

To start a kinetics run, the solvent was prepared at its consolute composition by weighing. Before mixing, the solvent and the reactant were placed in the water bath and allowed to come to thermal equilibrium. In those cases where the thermostat temperature lay in the two-phase region of the mixture, introduction of the reactant into the solvent produced immediate turbidity. Upon settling for 15 s, a meniscus appeared. The conductivity probe was inserted in the upper liquid layer. Between measurements of the conductivity, the probe was used to stir the reaction mixture so as to guarantee continuous equilibrium across the phase boundary. The time sequence of the conductivity measurements followed the method of Guggenhein.[23] The delay time Δ, separating measurements at times, t and $t + \Delta$, was approximately 2−2.5 half-lives or 20−30 min. Because the reaction was first order in the concentration of RX, the two sets of conductivity measurements $\sigma(t)$ and $\sigma(t + \Delta)$ could be combined in the equation

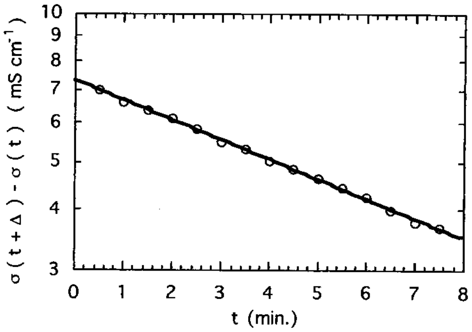

Figure 1. Guggenheim plot of conductivity data according to eq 2 for the hydrolysis of 150 μL of *tert*-amyl chloride in 25 mL of 38.8 wt % isobutyric acid + water at 36.80 °C. The conductivities $\sigma(t)$ and $\sigma(t + \Delta)$ are in the units mS cm^{-1}, while the time t is in minutes and the delay time, $\Delta = 20$ min, is about 2.1 half-lives.

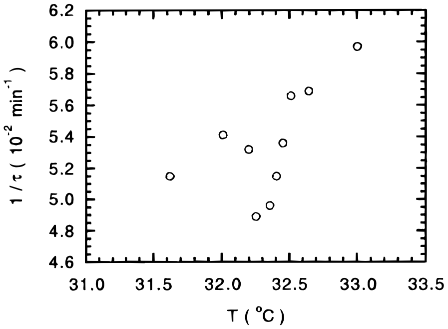

Figure 2. Specific rate of hydrolysis $1/\tau$ of *tert*-amyl chloride in isobutyric acid + water as a function of temperature T. The upper consolute temperature of the equilibrium mixture occurs at 32.3 °C. See the first line of Table 1 for specification of the mixture.

$$\ln[\sigma(t + \Delta) - \sigma(t)] = \ln[\sigma_{\mathrm{HX}}(1 - \mathrm{e}^{-\Delta/\tau})] - t/\tau \qquad (2)$$

where σ_{HX} is the conductivity of the acid at equilibrium and τ is the relaxation time (inverse of the first-order rate constant) for the reaction. As illustrated by Figure 1, plots of the left hand side of eq 2 as a function of t produced good straight lines with negative slope. The value of τ was computed from the slope.

After repetition of the above procedure at various temperatures, the values of $1/\tau$ were plotted as shown in Figures 2−7.

Discussion and Conclusions

As demonstrated in each of Figures 2−7, there is a suppression in the specific reaction rate, $1/\tau$, within a few tenths °C on either side of the critical point. The effect is independent of both the reaction and the solvent pair and occurs at the UCST (Figures 2 and 3), as well as the LCST (Figures 4−6).

In a separate experiment, reported in the Figure 7, we measured the rate of hydrolysis of 150 μL of *tert*-amyl chloride added to 25 mL of isobutyric acid + water. As the critical temperature depends upon the amount of reactant, this mixture had an UCST at 36.46 °C. For this mixture, we observed a

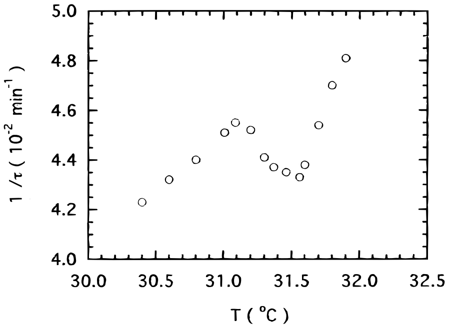

Figure 3. Specific rate of hydrolysis $1/\tau$ of *tert*-butyl chloride in isobutyric acid + water as a function of temperature *T*. The upper consolute temperature of the equilibrium mixture occurs at 31.55 °C. See the second line of Table 1 for specification of the mixture.

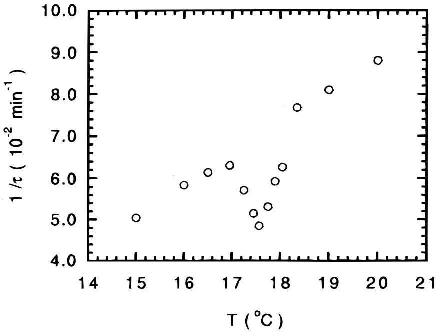

Figure 4. Specific rate of hydrolysis $1/\tau$ of *tert*-butyl bromide in triethylamine + water as a function of temperature *T*. The lower consolute temperature of the equilibrium mixture occurs at 17.6 °C. See the third line of Table 1 for specification of the mixture.

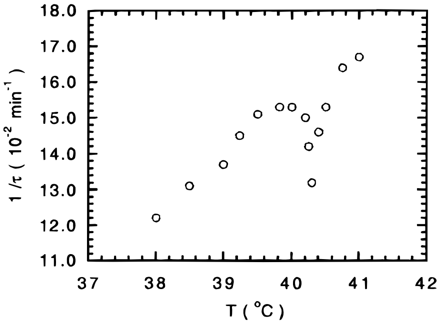

Figure 5. Specific rate of hydrolysis $1/\tau$ of 3-chloro-3-methylpentane in 2-butoxyethanol + water as a function of temperature *T*. The lower consolute temperature of the equilibrium mixture occurs at 40.35 °C. See the fourth line of Table 1 for specification of the mixture.

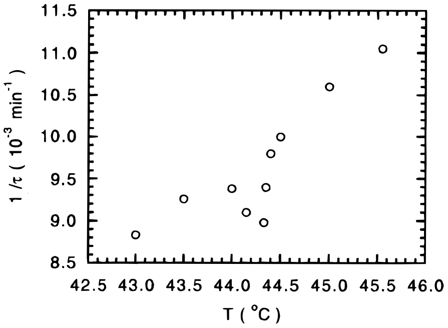

Figure 6. Specific rate of hydrolysis $1/\tau$ of 4-methylbenzylbromide in 2-butoxyethanol + water as a function of temperature *T*. The lower consolute temperature of the equilibrium mixture occurs at 44.3 °C. See the fifth line of Table 1 for specification of the mixture.

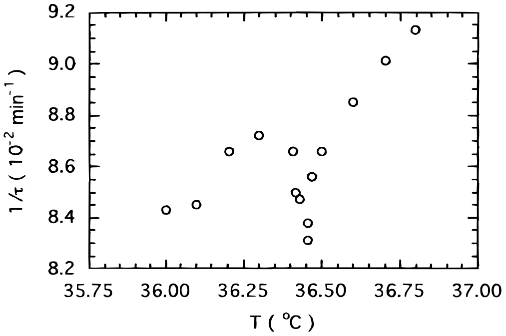

Figure 7. Specific rate of hydrolysis $1/\tau$ for 150 μL of *tert*-amyl chloride in 25 mL of 38.8 wt % isobutyric acid + water. The upper consolute temperature of the equilibrium mixture occurs at 36.46 °C.

suppression in the specific rate centered on 36.46 °C. When combined with the results shown in Figure 2 and Table 1, this observation demonstrates that as far as critical slowing down is concerned, any point along the critical line is the same as any other.

According to theory, $1/\tau$, should be proportional to the thermodynamic derivative, $(\partial\Delta G_1/\partial\xi)_e$, where ΔG_1 is the instantaneous Gibbs free energy differences between products and reactants in eq 1, ξ is the extent of reaction, and the subscript *e* implies that the derivative is evaluated at thermodynamic equilibrium.[24] We demonstrate the applicability of this theory to our data in the Appendix.

An analysis of the temperature dependence $(\partial\Delta G_1/\partial\xi)_e$ begins with a determination of the number of thermodynamic variables. For simplicity of argument, we shall consider for the moment the reaction taking place in the single-phase region of the phase diagram, where all components are miscible. Let X_{RX}, X_{HOH}, X_{ROH}, X_{HX}, and X_{I} be the mole fractions describing the composition, where X_{I} is the mole fraction of the inert component. The remaining relevant variables are temperature and pressure. The total number of thermodynamic variables describing the system is thus seven.

Not all of these are independent, however. Because eq 1 conserves moles, X_{I} is a constant. Furthermore, the stoichiometry dictates that $X_{\mathrm{ROH}} = X_{\mathrm{HX}}$, while the sums $X_{\mathrm{RX}} + X_{\mathrm{ROH}}$, and $X_{\mathrm{HOH}} + X_{\mathrm{HX}}$, respectively, must each be constant. To specify equilibrium, we must also have $\Delta G_1 = 0$. Hence, there exist five constraints on the seven thermodynamic variables.

There remain thus only two thermodynamically independent variables. These are the pressure and the temperature. The former equals 1 atm, while the latter is specified by the thermostat. According to Griffiths and Wheeler,[25] because none of the mole fractions are independent, we can expect $((\partial\Delta G_1/\partial\xi)_e$ to approach zero and, hence, $1/\tau$ to diminish as *T* nears T_c. This prediction is confirmed by Figures 2−7.

In the argument above, we have assumed that all components were miscible. Nonetheless, when, as in the case of many of our experiments, two phases were present, our conclusions are unchanged, since there were then 14 variables and 12 constraints, and the independent variables continue to be only temperature and pressure.

One must also consider side reactions, such as the loss of Cl^- by *tert*-amyl chloride to form 2-methylbutene-2 or 2-methylbutene-1. None of these can change the count of independent variables, however, since with the introduction of each new chemical component, there comes an additional constraint equation associated with the reaction which forms it.

We thus conclude on the basis of Figures 2−7 that the rates of hydrolysis reactions are suppressed near the consolute points of liquid mixtures. The effect occurs at both upper and lower critical solution temperatures. As demonstrated by comparing Figures 2 and 7, this slowing down phenomenon follows the shift in critical temperature caused by a change in the initial concentration of the reactant, proving that all points along the critical line are equivalent. Moreover, so long as the hydrolysis rate is first order, the slowing down appears to be independent of the chemical natures of both the reactant and the solvent pair.

Acknowledgment. This research was sponsored in part by the Donors of the Petroleum Research Fund, administered by the American Chemical Society, and in part by the National Aeronautics and Space Administration through Contract NAGW 812 with the Consortium for Materials Development in Space of the University of Alabama in Huntsville. The authors thank Dr. Susan Hill for help in the preparation of the figures.

Appendix

In its simplest form, the mechanism of the S_N1 hydrolysis reaction,

$$\mathrm{RX} + \mathrm{HOH} \rightarrow \mathrm{ROH} + \mathrm{HX} \qquad (A.1)$$

can be represented by the two elementary steps:

$$\mathrm{RX} \rightarrow \mathrm{R}^+ + \mathrm{X}^- \qquad (A.2)$$

$$\mathrm{R}^+ + \mathrm{HOH} \rightarrow \mathrm{ROH} + \mathrm{H}^+ \qquad (A.3)$$

The rate controlling reaction is eq A.2, while eq A.3 is fast and essentially at instantaneous equilibrium.[23]

For the case of a dilute ideal solution, we let κ_2' and κ_2'' be the rate coefficients for eq A.2 in the forward and reverse directions, respectively, while κ_3' and κ_3'' are the corresponding coefficients for eq A.3. To take into account solvent effects, we write the net rate r_2 of eq A.2 in the forward direction as[23]

$$r_2 = \frac{\kappa_2' y_{\mathrm{RX}} c_{\mathrm{RX}}}{y_2^*} - \frac{\kappa_2'' y_{\mathrm{R}^+} y_{\mathrm{X}^-} c_{\mathrm{R}^+} c_{\mathrm{X}^-}}{y_2^*} \qquad (A.4)$$

where c_{RX}, c_{R^+}, and c_{X^-} are the concentrations of the species RX, R^+, and X^-, while y_{RX}, y_{R^+}, y_{X^-}, and y_2^* are the activity coefficients of these species and the transition state, respectively. If we let the corresponding thermodynamic activities be a_{RX}, a_{R^+}, and a_{X^-}, eq A.4 can be rewritten in the form[26]

$$r_2 = \frac{\kappa_2' a_{\mathrm{RX}}}{y_2^*} - \frac{\kappa_2'' a_{\mathrm{R}^+} a_{\mathrm{X}^-}}{y_2^*} \qquad (A.5)$$

An analogous treatment of eq A.3 leads to

$$r_3 = \frac{\kappa_3' a_{\mathrm{R}^+} a_{\mathrm{HOH}}}{y_3^*} - \frac{\kappa_3'' a_{\mathrm{ROH}} a_{\mathrm{H}^+}}{y_3^*} \qquad (A.6)$$

Equation A.5 can be factored to assume the form

$$r_2 = \frac{\kappa_2' a_{\mathrm{RX}}}{y_2^*}\left[1 - \frac{\kappa_2''}{\kappa_2'} \frac{a_{\mathrm{R}^+} a_{\mathrm{X}^-}}{a_{\mathrm{RX}}}\right] \qquad (A.7)$$

According to the steady state approximation, we can set $r_3 = 0$. This permits eq A.6 to be solved for

$$a_{\mathrm{R}^+} = \frac{\kappa_3''}{\kappa_3'} \frac{a_{\mathrm{ROH}} a_{\mathrm{H}^+}}{a_{\mathrm{HOH}}} \qquad (A.8)$$

Upon substitution of eq A.8 into eq A.7, we obtain

$$r_2 = \frac{\kappa_2' a_{\mathrm{RX}}}{y_2^*}\left[1 - \frac{\kappa_2''}{\kappa_2'} \frac{\kappa_3''}{\kappa_3'} \frac{a_{\mathrm{ROH}} a_{\mathrm{HX}}}{a_{\mathrm{RX}} a_{\mathrm{HOH}}}\right] \qquad (A.9)$$

where we have set $a_{\mathrm{HX}} = a_{\mathrm{H}^+} a_{\mathrm{X}^-}$. Considering both eqs A.5 and A.6 at equilibrium leads to

$$\frac{\kappa_2'}{\kappa_2''} = \exp(-\Delta G_2^\circ/RT) \qquad (A.10)$$

and

$$\frac{\kappa_3'}{\kappa_3''} = \exp(-\Delta G_3^\circ/RT) \qquad (A.11)$$

where ΔG_2° and ΔG_3° are the respective standard free energies of reaction, R is the gas law constant, and T is the absolute temperature. The instantaneous free energy difference between products and reactants in the overall reaction represented by eq A.1 is

$$\Delta G_1 = \Delta G_1^\circ + RT \ln\left(\frac{a_{\mathrm{ROH}} a_{\mathrm{HX}}}{a_{\mathrm{RX}} a_{\mathrm{HOH}}}\right) \qquad (A.12)$$

where, because ΔG_1 is a state function,

$$\Delta G_1^\circ = \Delta G_2^\circ + \Delta G_3^\circ \qquad (A.13)$$

If we substitute eq A.12 into eq A.9 and use eqs A.10, A.11, and A.13, we find

$$r_2 = \frac{\kappa_2' a_{\mathrm{RX}}}{y_2^*}[1 - \exp(\Delta G_1/RT)] \qquad (A.14)$$

which is an equation relating the velocity of the rate determining step to the overall instantaneous free energy of reaction, ΔG_1. We can define the extent of reaction, ξ, by $\xi = c_{\mathrm{H}^+} = c_{\mathrm{X}^-}$. Expanding eq A.14 about $\xi = \xi_e$, where ξ_e is the equilibrium value of ξ, and $\Delta G_1(\xi_e) = 0$, we obtain

$$r_2 = -\frac{\kappa_2' a_{\mathrm{RX}}(\xi_e)}{y_2^*(\xi_e)RT}\left(\frac{\partial \Delta G_1}{\partial \xi}\right)_e (\xi - \xi_e) \qquad (A.15)$$

which is correct up to first order in $(\xi - \xi_e)$. Equation A.15 defines the relaxation rate,

$$\frac{1}{\tau} = \frac{\kappa_2' a_{\mathrm{RX}}(\xi_e)}{y_2^*(\xi_e)\mathrm{RT}}\left(\frac{\partial \Delta G_1}{\partial \xi}\right)_e \qquad (A.16)$$

Experimentally, the kinetics appear to be first order with the rate of formation of HX given by

$$r_2 = k_{\mathrm{obs}}(c - \xi) \qquad (A.17)$$

where c is the initial value of c_{RX} and k_{obs} is the observed rate constant. Equation A.17 implies that eq A.2 goes to completion,[23] so we can write approximately $c \simeq \xi_e$, from which we obtain

$$r_2 = -k_{\mathrm{obs}}(\xi - \xi_e) \qquad (A.18)$$

Comparing eqs A.15 and A.18, we have approximately $k_{\mathrm{obs}} \simeq$

$1/\tau$. This result is the basis for analyzing our experiments using eq A.16, where $1/\tau \sim (\partial \Delta G_1/\partial \xi)_e$.

References and Notes

(1) Toriumi, T. T.; Sakai, J.; Kawakami, T.; Osawa, D.; Azuma, M. *J. Soc. Ind. Jpn.* **1946**, *49*, 1.

(2) Krichevskii, I. R.; Tsekhanskaya, Yu. V. *Inzh.−Fiz. Zh.* **1962**, *5*, 104.

(3) Krichevskii, I. R.; Tsekhanskaya, Yu. V.; Polyakova, Z. A. *Russ. J. Phys. Chem.* **1966**, *40*, 715.

(4) Krichevskii, I. R.; Tsekhanskaya, Yu. V.; Rozhonovskaya, L. N. *Russ. J. Phys. Chem.* **1969**, *43*, 1393.

(5) Narayan, R.; Antal, M. J., Jr. *J. Am. Chem. Soc.* **1990**, *112*, 1927.

(6) Zagrobleny, J. A.; Bright, F. V. *J. Am. Chem. Soc.* **1993**, *115*, 701.

(7) Brennecke, D. L.; Tomasko, D. L.; Reshkin, J.; Eckert, C. A. *J. Phys. Chem.* **1990**, *94*, 7692.

(8) Eckert, C. A.; Knutson, B. L. *Fluid Phase Equilib.* **1993**, *83*, 13.

(9) Fernandez-Prini, R.; Japas, M. L. *Chem. Soc. Rev.* **1994**, *155*.

(10) Procaccia, I.; Gitterman, M. J. *J. Chem. Phys.* **1983**, *78*, 5275.

(11) Myers, D. B.; Smith, R. A.; Katz, J.; Scott, R. L. *J. Phys. Chem.* **1966**, *70*, 3341.

(12) Wheeler, J. C. *Phys. Rev. A* **1984**, *30*, 648.

(13) Milner, S. T.; Martin, P. C. *Phys. Rev. A* **1986**, *33*, 1996.

(14) Greer, S. C. *Int. J. Thermophys.* **1988**, *9*, 761.

(15) Gitterman, M. *J. Stat. Phys.* **1990**, *58*, 707.

(16) Tveekrem, J. L.; Cohn, R. H.; Greer, S. C. *J. Chem. Phys.* **1987**, *86*, 3602.

(17) Snyder, R. B.; Eckert, C. A. *AIChE. J.* **1973**, *19*, 1126.

(18) Muller, C.; Steiger, A.; Becker, F. *Thermochem. Acta* **1989**, *86*, 3602.

(19) Stein, A.; Allen, G. F. *J. Chem. Phys.* **1973**, *59*, 6079.

(20) Counsell, J. F.; Everett, D. H.; Munn, R. J. *Pure Appl. Chem.* **1961**, *2*, 335.

(21) Copp, J. L.; Everett, D. H. *Discuss. Faraday Soc.* **1953**, *15*, 174.

(22) Hales, B. J.; Bertrand, G. L.; Hepler, L. G. *J. Phys. Chem.* **1966**, *70*, 3470.

(23) Matthews, G. P. *Experimental Physical Chemistry*; Clarendon Press: Oxford, 1985.

(24) Castellan, G. W. *Ber. Bunsen-Ges.* **1963**, *67*, 989.

(25) Griffiths, R. B.; Wheeler, J. C. *Phys. Rev. A* **1970**, *2*, 1047.

(26) Haase, R. *Z. Phys. Chem.* **1987**, *153*, 217.